



Novel Mps1 kinase inhibitors: From purine to pyrrolopyrimidine and quinazoline leads



Matthew G. Bursavich^{a,*}, David Dastrup^a, Mark Shenderovich^a, Kraig M. Yager^a, Daniel M. Cimbora^b, Brandi Williams^b, D. Vijay Kumar^a

^a Medicinal Chemistry, Myrexis, Inc., 305 Chipeta Way, Salt Lake City, UT 84108, United States

^b In Vitro Pharmacology, Myrexis, Inc., 305 Chipeta Way, Salt Lake City, UT 84108, United States

ARTICLE INFO

Article history:

Received 9 September 2013

Revised 30 September 2013

Accepted 4 October 2013

Available online 11 October 2013

Keywords:

Mps1

TTK

Protein kinase inhibitors

Scaffold hopping

Conformational restriction

Structure-based design

Cancer

Purines

Pyrrolopyrimidines

Quinazoline

ABSTRACT

Mps1, also known as TTK, is a mitotic checkpoint protein kinase that has become a promising new target of cancer research. In an effort to improve the lead-likeness of our recent Mps1 purine lead compounds, a scaffold hopping exercise has been undertaken. Structure-based design, principles of conformational restriction, and subsequent scaffold hopping has led to novel pyrrolopyrimidine and quinazoline Mps1 inhibitors. These new single-digit nanomolar leads provide the basis for developing potent, novel Mps1 inhibitors with improved drug-like properties.

© 2013 Elsevier Ltd. All rights reserved.

Mps1, also known as TTK, is a dual specificity protein kinase that phosphorylates tyrosine, serine or threonine residues with a critical role during mitosis. Mps1 facilitates chromosomal alignment during metaphase, as well as proper attachment of the bipolar microtubules to the kinetochores by eliminating misattachments.^{1,2} It is also required for the full assembly of the spindle checkpoint proteins at the kinetochore and activation of this complex.³

Mps1 is dynamic kinase expressed only in proliferating cells and activated via phosphorylation during mitosis. It is over expressed in various human tumors and necessary for cellular proliferation. Mps1 inhibition has been shown to cause premature mitotic exit and gross aneuploidy, which is ultimately associated with cell death. It has been hypothesized that mitotic checkpoints are necessary to sustain cancer cellular proliferation in the presence of aneuploidy. Thus, Mps1 inhibition has become a promising new target of cancer research.

We have recently published our efforts developing purine based lead structures **1a**, **1b** and **2** as potent, selective, novel inhibitors of

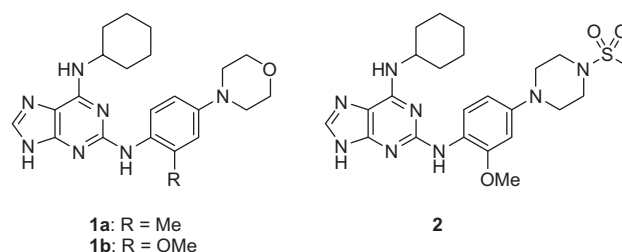


Figure 1. Myrexis Mps1 lead structures.

Mps1 (Fig. 1). Purine **1a** has been shown to disrupt the spindle assembly checkpoint, resulting in chromosome segregation defects and aneuploidy.^{4,5} Purine **1a** also demonstrated cytotoxicity across a broad panel of tumor cell lines and exhibited antitumor activity in nude mice bearing human tumor xenografts.⁴ Since we initiated our efforts, several promising Mps1 kinase inhibitors have been published (Fig. 2).⁶

Due to the high molecular weight (MW) and polar surface area (TPSA) of these leads (Table 1), a de novo design effort was undertaken. Herein we report those efforts leading to new pyrrolopyrimidine and quinazoline inhibitors of Mps1. These new analogs

* Corresponding author. Address: Envivo Pharmaceuticals, 500 Arsenal Street, Watertown, MA 02472, United States. Tel.: +1 617-225-4219.

E-mail address: mbursavich@envivopharma.com (M.G. Bursavich).

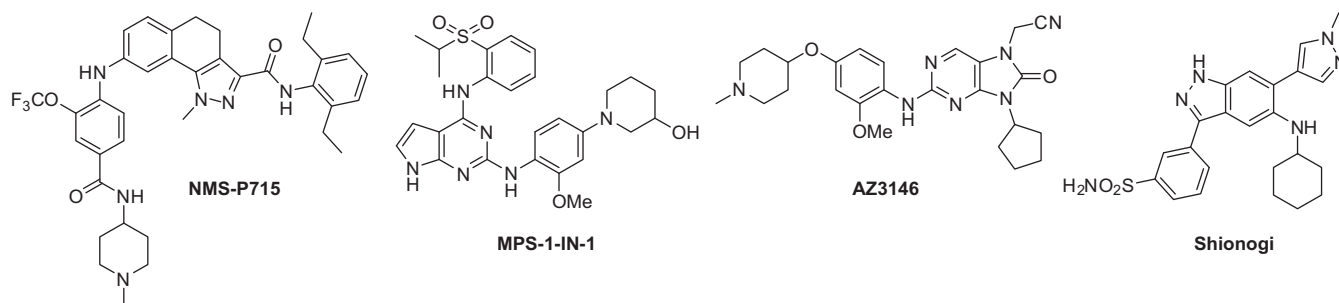
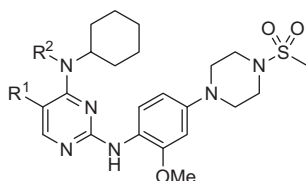


Figure 2. Published Mps1 kinase inhibitors.

Table 1
Structure–activity relationships of pyrimidines



Compd	R ¹	R ²	Mps1 ^a IC ₅₀ (nM)	HCT116 ^a IC ₅₀ (μM)	MW	TPSA	LE ^b
1a	–	–	5	0.023	424	100	0.27
2	–	–	2	0.011	501	137	0.25
6	H	H	>100	–	461	108	–
7	H	Me	35	2.0	475	99	0.23
8	Me	H	28	1.5	475	108	0.23
9	Me	Me	>100	–	489	99	–

^a Values are means of two experiments, standard deviations are ±10%.

^b LE = $-\text{Log}(\text{Mps1 IC}_{50})/\#$ of heavy atoms.

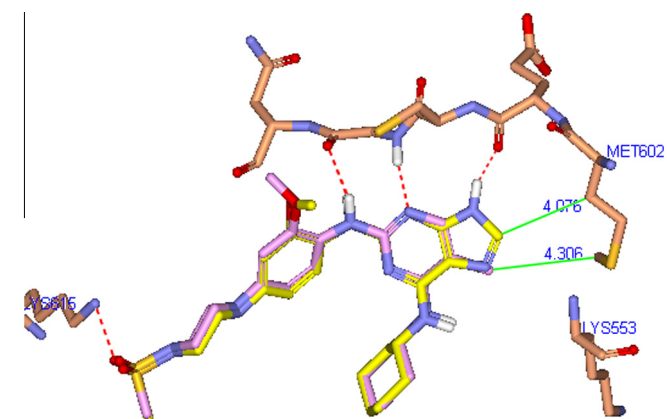
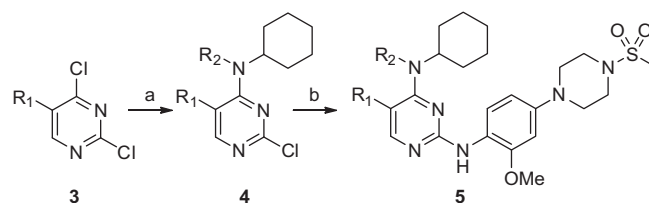


Figure 3. Binding model overlay with 5-methyl pyrimidine structure (pink) and Mps1 lead structure 2.

demonstrate potent Mps1 activity with significantly reduced TPSA while maintaining their ligand efficiency (LE).⁷

In an effort to reduce the MW and TPSA of the lead compounds, a series of pyrimidines were first designed and modeled. The binding model overlay of the 5-methyl pyrimidine scaffold with purine lead compound 2 is shown in Figure 3.⁸

The synthesis of the diaminopyrimidine inhibitors is shown in Scheme 1.⁹ The synthesis begins with commercially available 2,4-dichloropyrimidines 3 (R¹ = H or Me). Heating cyclohexyl amine or *N*-methylcyclohexylamine with 3 and triethylamine in THF at 50 °C provided compound 4 (R¹ = H or Me; (R² = H or Me).



Scheme 1. Reagents and conditions: (a) amine, TEA, THF 50 °C; (b) aniline, cat. TsOH, dioxane, 170 °C, MW.

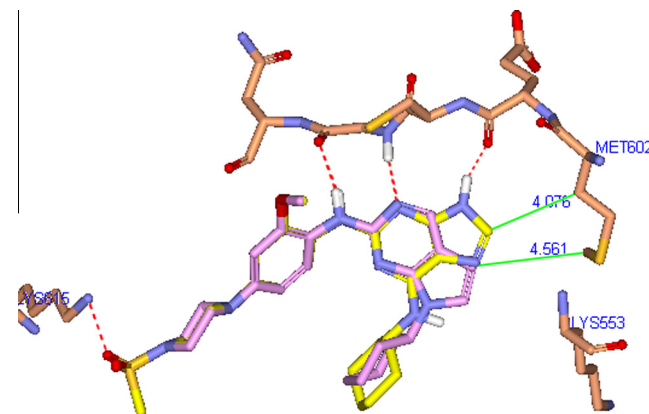
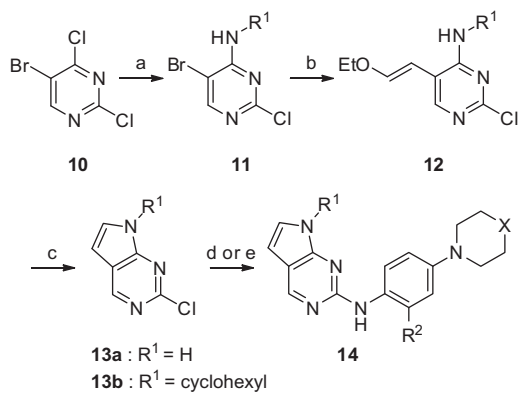


Figure 4. Binding model overlay with *N*-cyclohexyl pyrrolopyrimidine structure (pink) and Mps1 lead structure 2.

Reaction of 4 with the desired aniline under catalytic acid conditions in the microwave provided the diaminopyrimidines 5.¹⁰



Scheme 2. Reagents and conditions: (a) ammonia, THF or cyclohexylamine, THF, 50 °C (b) $B(OH)_2CHCHOEt$, $NaHCO_3$, $Pd(PPh_3)_4$, DME, reflux; (c) AcOH, 120 °C; (d) (i) Ar/HetArBr, CuI, K_3PO_4 , (\pm)-*trans*-1,2-diaminocyclohexane, 90 °C; (ii) aniline, Cs_2CO_3 , $Pd(OAc)_2$, BINAP, toluene, reflux; (e) aniline, Cs_2CO_3 , $Pd(OAc)_2$, BINAP, toluene, reflux.

Kinase inhibition activity was determined as previously described using full-length Mps1 enzyme at 2xKm ATP concentrations. Cellular proliferation activity was determined by monitoring cell growth densities in HCT116 cell cultures.⁴

The importance of combined R^1 , R^2 substituents was immediately evident. The unsubstituted compound (**6**: R^1 , R^2 = H) was shown to be inactive, but substitution of an R^2 methyl group (**7**) provided a potent starting point (IC_{50} = 35 nM). Incorporating an R^1 methyl group on the pyrimidine ring with an unsubstituted R^2 group (**8**) provided a slightly more potent analog (IC_{50} = 28 nM). While **7** and **8** are not as potent as purine **2**, these analogs possess reduced MW, reduced TPSA, and only slightly reduced LE as compared with purine lead **2**. Interestingly, the disubstituted compound (**9**: R^1 , R^2 = Me) was shown to be inactive, presumably due to an unproductively biased conformation.

Encouraged by the diaminopyrimidine results, and realizing the potential for conformational restriction, a series of pyrrolopyrimidines were designed and modeled. The binding model overlay of the *N*-cyclohexyl pyrrolopyrimidine scaffold with purine lead compound **2** is shown in Figure 4.⁸

The synthesis of the pyrrolopyrimidine inhibitors⁹ (Scheme 2) begins with reaction of commercially available 5-bromo-2,4-dichloropyrimidine **10** with either ammonia or cyclohexylamine to provide **11**. Suzuki reaction with the vinyl ether borane reagent provided the pyrrolopyrimidine precursor **12**.¹¹ Cyclization under acidic conditions afforded both **13a** and **13b**. Conversion of **13a**

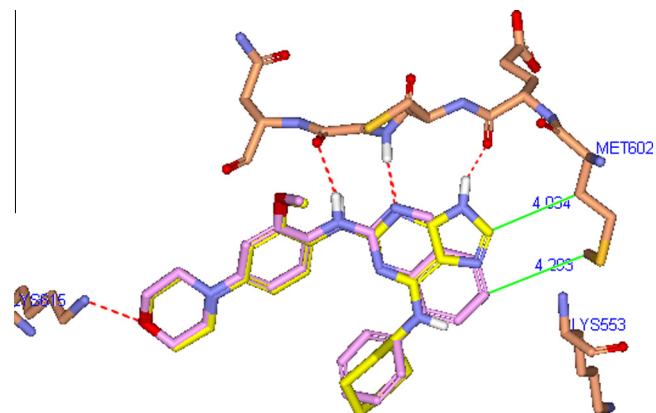
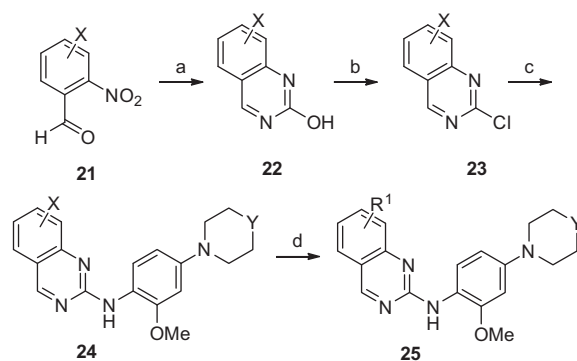


Figure 5. Binding model overlay with quinazoline structure (pink) and Mps1 lead structure **1b**.

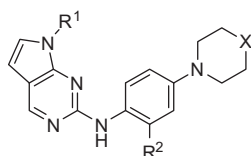


Scheme 3. Reagents and conditions: (a) (i) Fe, AcOH, HCl, EtOH, 70 °C; (ii) urea, 180 °C; (b) $POCl_3$, 110 °C; (c) aniline–HCl, IPA, 100 °C; (d) Ar/HetArB(OH)₂, Na_2CO_3 , $Pd(PPh_3)_4$, DME or cyclohexylamine, Cs_2CO_3 , $Pd(OAc)_2$, BINAP, toluene, reflux.

(R^1 = H) into **14** required an initial Buchwald reaction to functionalize the indole NH and introduce the R^1 substituent followed by a second Buchwald–Hartwig reaction to incorporate the desired aniline.^{12,13} Conversion of **13b** (R^1 = cyclohexyl) into **14** required the same Buchwald–Hartwig reaction to install the desired aniline.¹³

In the case of the pyrrolopyrimidines (Table 2) all the R^1 = cyclohexyl analogs (**15–17**) were shown to be potent Mps1 inhibitors. The 2-methyl-morpholine analog **16** (R^2 = Me, X = O) provided an attractive starting point (IC_{50} = 22 nM) with a MW under 400, TPSA

Table 2
Structure–activity relationships of pyrrolopyrimidines

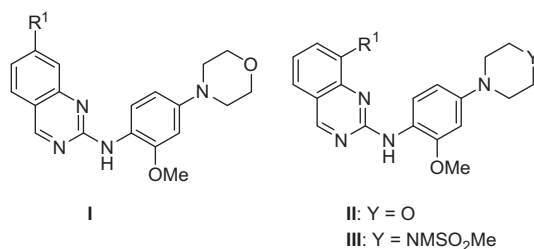


Compd	R^1	R^2	X	Mps1 ^a IC_{50} (nM)	HCT116 ^a IC_{50} (μ M)	MW	TPSA	LE ^b
15	Cyclohexyl	OMe	O	46	7.5	408	64	0.24
16	Cyclohexyl	Me	O	22	8.6	392	55	0.26
17	Cyclohexyl	OMe	NSO ₂ Me	20	0.75	485	101	0.23
18	Phenyl	OMe	NSO ₂ Me	>100	–	479	101	–
19	2-Pyridyl	OMe	NSO ₂ Me	32	10	480	114	0.22
20	3-Pyridyl	OMe	NSO ₂ Me	>100	–	480	114	–

^a Values are means of two experiments, standard deviations are $\pm 10\%$.

^b LE = $-\log(Mps1 IC_{50})/\#$ of heavy atoms.

Table 3
Structure–activity relationships of quinazolines



Compd	Scaffold	R ¹	Mps1 ^a IC ₅₀ (nM)	HCT116 ^b IC ₅₀ (μM)	MW	TPSA	LE ^b
26	I	Phenyl	>100	–	412	60	–
27	I	<i>N</i> -Cyclohexyl	>100	–	434	72	–
28	II	Phenyl	12	0.85	412	60	0.26
29	II	<i>N</i> -Cyclohexyl	9	6.32	434	72	0.25
30	III	Phenyl	5	1.74	490	96	0.25
31	III	3-Pyridyl	8	1.58	491	109	0.24
32	III	<i>N</i> -Cyclohexyl	2	0.81	511	108	0.25

^a Values are means of two experiments, standard deviations are ±10%.

^b LE = –Log(Mps1 IC₅₀)/# of heavy atoms.

of 55, and a LE slightly better than purine lead **2** (LE = 0.26 vs 0.25). The 2-methoxy-4-sulfonamide analog **17** (R² = Me, X = NSO₂Me) also provided a potent starting point (IC₅₀ = 20 nM) demonstrating submicromolar cellular toxicity, reduced MW and TPSA compared to purine **2** (TPSA = 101 vs 137). In the case of the R¹ = aryl or heteroaryl groups (**18–20**), both the phenyl and 3-pyridyl analogs were shown to be substantially less active. The 2-pyridyl analog **19** was shown to be slightly less active against Mps1 than the cyclohexyl analog (compare **17** vs **19**), but maintained acceptable TPSA and LE values, while the phenyl and 3-pyridyl analogs demonstrated IC₅₀s >100 nM.

Based on the encouraging results with the pyrrolopyrimidines, a series of quinazolines were designed and modeled. The binding model overlay of the phenyl quinazoline scaffold with purine lead compound **1b** is shown in Figure 5.⁸

The synthesis of the quinazolines inhibitors⁹ (Scheme 3) begins with commercially available halo-nitrophenyl aldehydes **21** (X = 6-Br or 5-Cl). Iron reduction of the nitro group of **21** and subsequent cyclization with urea provided intermediate **22**. Treatment of **22** with POCl₃ afforded the chloroquinazoline **23**. Displacement of the pyrimidinyl chloride with desired aniline under acidic conditions provided compound **24**.¹⁰ Finally, a Buchwald reaction¹² to install an R¹ amine substituent or Suzuki reaction to incorporate an R¹ aryl or heteroaryl group provided the desired quinazoline inhibitors **25**.

While scaffold I analogs (**26** and **27**) were shown to be inactive, the regioisomeric scaffold II and III analogs were much more promising (Table 3). The R¹ = phenyl analog **28** provided a potent starting point (IC₅₀ = 12 nM) with submicromolar cellular toxicity, reduced MW and TPSA (TPSA = 60 vs 137), and similar LE compared to purine lead compound **1b**. The R¹ = *N*-cyclohexyl analog **29** provided a further boost in biochemical potency (IC₅₀ = 9 nM) with a slightly increased MW, reduced TPSA, and similar LE compared to purine lead compound **1b**. All three of the scaffold III compounds possessing the aniline sulfonamide substituent (**30–32**) showed single digit nanomolar Mps1 potency with slightly decreased or similar MW, reduced TPSA, and similar LE compared to purine lead compound **2**. Compound **32** also demonstrated submicromolar cellular toxicity.

In conclusion, we have presented a series of novel Mps1 inhibitors identified via de novo design efforts on a purine-based lead scaffold. Structure design using molecular modeling, followed by

conformational restriction and scaffold hopping led to new pyrrolopyrimidine and quinazoline inhibitors. These new scaffolds have been shown to be potent Mps1 inhibitor starting points with lowered MW, TPSA, and good ligand efficiencies compared to the purine leads. Some of the analogs also possess submicromolar cellular cytotoxicity. These new leads provide the basis for developing more potent, novel inhibitors of Mps1 with drug-like properties.

Acknowledgement

We thank the Myrex Analytical Department for their help with compound purification and characterization.

References and notes

- Jelluma, N.; Brenkman, A. B.; van den Broek, N. J.; Crujnsen, C. W.; van Osch, M. H.; Lens, S. M.; Medema, R. H.; Kops, G. J. *Cell* **2008**, *132*, 233.
- Huang, H.; Hittle, J.; Zappacosta, F.; Annan, R. S.; Hershko, A.; Yen, T. J. *J. Cell Biol.* **2008**, *183*, 667.
- Liu, S. T.; Chan, G. K.; Hittle, J. C.; Fujii, G.; Lees, E.; Yen, T. J. *Mol. Biol. Cell* **2003**, *14*, 1638.
- Tardiff, K. D.; Roger, A.; Cassiano, J.; Roth, B. L.; Cimbora, D. M.; McKinnon, R.; Peterson, A.; Douce, T.; Robinson, R.; Dorweiler, I.; Davis, T.; Hess, M. A.; Ostanin, K.; Papac, D. I.; Baichwal, V.; McAlexander, I.; Willardson, J. A.; Saunders, M.; Hoarau, C.; Kumar, D. V.; Wettstein, D. A.; Carlson, R. O.; Williams, B. L. *Mol. Cancer Ther.* **2011**, *10*, 2267.
- Kumar, D. V.; Hoarau, C.; Bursavich, M.; Slattum, P.; Gerrish, D.; Yager, K.; Saunders, M.; Shenderovich, M.; Roth, B.; McKinnon, R.; Chan, A.; Cimbora, D.; Reeves, L.; Patton, S.; Bradford, C.; Papac, D.; Williams, B.; Carlson, R. O. *Bioorg. Med. Chem. Lett.* **2012**, *22*, 4377.
- (a) Caldarelli, M.; Angiolini, M.; Disingrini, T.; Donati, D.; Guanci, M.; Nuvoloni, S.; Poster, H.; Quartieri, F.; Silvagni, M.; Colombo, R. *Bioorg. Med. Chem. Lett.* **2011**, *21*, 4507; (b) Kwiatkowski, N.; Jelluma, N.; Fillippakopoulos, P.; Soundararajan, M.; Manak, M. S.; Kwon, M.; Choi, H. G.; Sim, T.; Deveraux, Q. L.; Rottmann, S.; Pellman, D.; Shah, J. V.; Kops, G. J. P. L.; Knapp, S.; Gray Nat, N. S. *Chem. Biol.* **2010**, *6*, 359; (c) Hewitt, L.; Tighe, A.; Santaguida, S.; White, A. M.; Jones, C. D.; Musacchio, A.; Green, S.; Taylor, S. S. *J. Cell Biol.* **2010**, *190*, 25; (d) Kusakabe, K.; Ide, N.; Daigo, Y.; Tachibana, Y.; Itoh, T.; Yamamoto, T.; Hashizume, H.; Hato, Y.; Higashino, K.; Okano, Y.; Sato, Y.; Inoue, M.; Iguchi, M.; Kanazawa, T.; Ishioka, Y.; Dohi, K.; Kido, Y.; Sakamoto, S.; Yasuo, K.; Maeda, M.; Higaki, M.; Ueda, K.; Yoshizawa, H.; Baba, Y.; Shiota, T.; Murai, H.; Nakamura, Y. *J. Med. Chem.* **2013**, *56*, 4343.
- Abad-Zapatero, C.; Metz, J. T. *Drug Discovery Today* **2005**, *10*, 464.
- Molecular Docking Studies were Performed Using Schrodinger Program Glide: Glide5.0 User Manual*; Schrodinger Press, Schrodinger, LLC: New York, NY, **2008**; Crystal structure of Mps1 complex with a small molecule inhibitor (PDB ID 3H9F, Ref. 6) solved with resolution 2.60 Å was used as a target for docking. Docking model of Mps1 complex with compound **1** was further refined using Schrodinger induced fit docking protocol: Sherman, W.; Day, T.; Jacobson, M.

- P.; Friesner, R. A.; Farid, R. J. *Med. Chem.* **2006**, *49*, 534; *The Images were made with Accelrys Discovery Studio Visualizer, Release 3.2; Accelrys Software Inc.: San Diego, USA, 2011.*
9. All newly prepared compounds were purified by reverse phase HPLC and characterized by LCMS, NMR and HRMS.
10. Bursavich, M. G.; Lombardi, S.; Gilbert, A. M. *Org. Lett.* **2005**, *7*, 4113.
11. Whelligan, D. K. T.; Thomson, D. W.; Taylor, D.; Hoelder, S. J. *Org. Chem.* **2010**, *75*, 11.
12. Surry, D. S.; Buchwald, S. L. *Chem. Sci.* **2010**, *1*, 13.
13. Wolfe, J. P.; Buchwald, S. L. *J. Org. Chem.* **2000**, *65*, 1144.